Axonal-SMN (a-SMN), a protein isoform of the survival motor neuron gene, is specifically involved in axonogenesis

Veronica Setola*, Mineko Terao†, Denise Locatelli*, Stefania Bassanini*, Enrico Garattini†, and Giorgio Battaglia*‡

*Molecular Neuroanatomy Laboratory, Department of Experimental Neurophysiology and Epileptology, Istituto Neurologico ''C. Besta,'' via Celoria 11, 20133 Milano, Italy; and †Molecular Biology Laboratory, Centro Catullo e Daniela Borgomainerio, Istituto di Ricerche Farmacologiche ''Mario Negri,'' via Eritrea 62, 20157 Milano, Italy

Spinal muscular atrophy (SMA) is an autosomal recessive disease of childhood due to loss of the telomeric survival motor neuron gene, *SMN1*. The general functions of the main *SMN1* protein product, full-length SMN (FL-SMN), do not explain the selective motoneuronal loss of SMA. We identified axonal-SMN (a-SMN), an alternatively spliced *SMN* form, preferentially encoded by the *SMN1* gene in humans. The a-SMN transcript and protein are down-regulated during early development in different tissues. In the spinal cord, the a-SMN protein is selectively expressed in motor neurons and mainly localized in axons. Forced expression of a-SMN stimulates motor neuron axonogenesis in a time-dependent fashion and induces axonal-like growth in non-neuronal cells. Exons 2b and 3 are essential for the axonogenic effects. This discovery indicates an unexpected complexity of the *SMN* gene system and may help in understanding the pathogenesis of SMA.

alternative splicing | neurodegeneration | spinal muscular atrophy | intron retention | axonal sprouting

S pinal muscular atrophy (SMA) is an autosomal recessive disease of childhood causing selective motor neuron death. SMA is the leading genetic cause of infant mortality, with an incidence of 1:10,000 and a carrier frequency of 1:50 (1). The telomeric survival motor neuron gene (*SMN1*) is the SMA disease gene, and the duplicated centromeric gene, *SMN2*, governs the severity of the disease (2, 3). Current knowledge suggests that *SMN1* codes for a single functional protein [full-length SMN (FL-SMN)], and the major product of *SMN2* is Δ7-SMN (lacking the C terminus), an unstable protein of minor significance (4, 5).

The FL-SMN protein is expressed in the cytoplasm and nucleus of all cells (6, 7) and is involved in spliceosomal assembly and pre-mRNAs maturation (8–10). Other proposed roles include general cellular functions (11–15). How reduced FL-SMN levels lead to selective degeneration of motor neurons in SMA remains undetermined. FL-SMN may serve motor neuron-specific functions, perhaps interacting with partner proteins selectively expressed in these cells. However, these functions and the partner proteins are still not known. Additional protein products of the *SMN* genes have been postulated (16–19). The identification of SMN proteins acting specifically in motor neurons would be a major step forward in understanding SMA.

We identify and characterize an *SMN* transcript (GenBank accession no. AY876898) originating from the retention of *SMN* intron 3 and encoding the axonal-SMN (a-SMN) protein. In the spinal cord, a-SMN is selectively expressed in developing motor neurons and mainly localized in axons. This is confirmed by overexpression experiments in cultured cells. These also demonstrate the following: (*i*) a-SMN stimulates motor neuron axonogenesis in a time-dependent fashion, and (*ii*) a-SMN induces axonal-like growth in non-neuronal cells such as HeLa. The specific localization and function suggest a role in motor neurons. Because human a-SMN is a specific product of the *SMN1* gene, its loss may be a determinant of SMA.

Results

Identification of an *SMN* Transcript in the Rat Spinal Cord.
To search for new *SMN* transcripts, we analyzed the poly(A)+ RNA fraction of rat spinal cords with RACE/PCR and nested primers against exons 1 and 3. We isolated SMN cDNAs containing the entire sequence of intron 3, beside cDNAs consisting of the fully spliced form of FL-SMN (data not shown). The intron 3-containing transcript was named a-SMN.

We defined the molecular structure of a-SMN mRNA in the poly(A)+ RNA fraction of rat spinal cord. On Northern blot analysis, an intron 3 cDNA probe revealed a specific transcript similar in size to the FL-SMN counterpart (Fig. 1a). These results were supported by RNase protection assays. An antisense RNA corresponding to a genomic sequence encompassing intron 2b, exon 3, intron 3, and exon 4 protected three fragments, originating from exons 3 and 4 of the FL-SMN mRNA, and the exon 3/intron 3/exon 4 sequence of the a-SMN mRNA. Thus, the a-SMN transcript originates from the same genomic DNA strand encoding the FL-SMN mRNA and is also developmentally regulated (Fig. 1b). RT-PCR experiments with intron 3- and exon 1- or exon 8-primers (Fig. 1 c and d) indicated that the a-SMN transcript extends to exon 1 in the 5′ direction and to exon 8 in the 3′ direction. The presence of intron 3 in a-SMN was confirmed by the fact that (*i*) exon 3- and exon 4-primers amplified two DNA fragments corresponding to a-SMN mRNA, which retains the intron 3 sequence, and FL-SMN mRNA (Fig. 1c); and (*ii*) competitive PCR experiments with exon 3- and intron 3-/exon 6-primers indicated the presence of the FL-SMN and a-SMN transcripts. The latter mRNA was selectively down-regulated from embryonic day 15 to postnatal day 15 compared with the FL-SMN counterpart (Fig. 1e).

These experiments indicate that the a-SMN mRNA accounts for only a small fraction of the total pool of *SMN* transcripts and is down-regulated during spinal cord development. Thus, the a-SMN transcript (Fig. 1h) is expressed mainly during the crucial phases of motoneuronal maturation, declining in adulthood.

RACE-PCR and RT-PCR experiments were also conducted on the poly(A)+ RNA fraction of human spinal cord and the NB4 human myeloid cell line. RT-PCR experiments demonstrated the existence of the a-SMN transcript in humans, too (Fig. 1 f and g). 3′-RACE-PCR experiments with intron 3-nested primers indicated that the human a-SMN mRNA is preferentially encoded by the

© 2007 by The National Academy of Sciences of the USA

NEUROSCIENCE
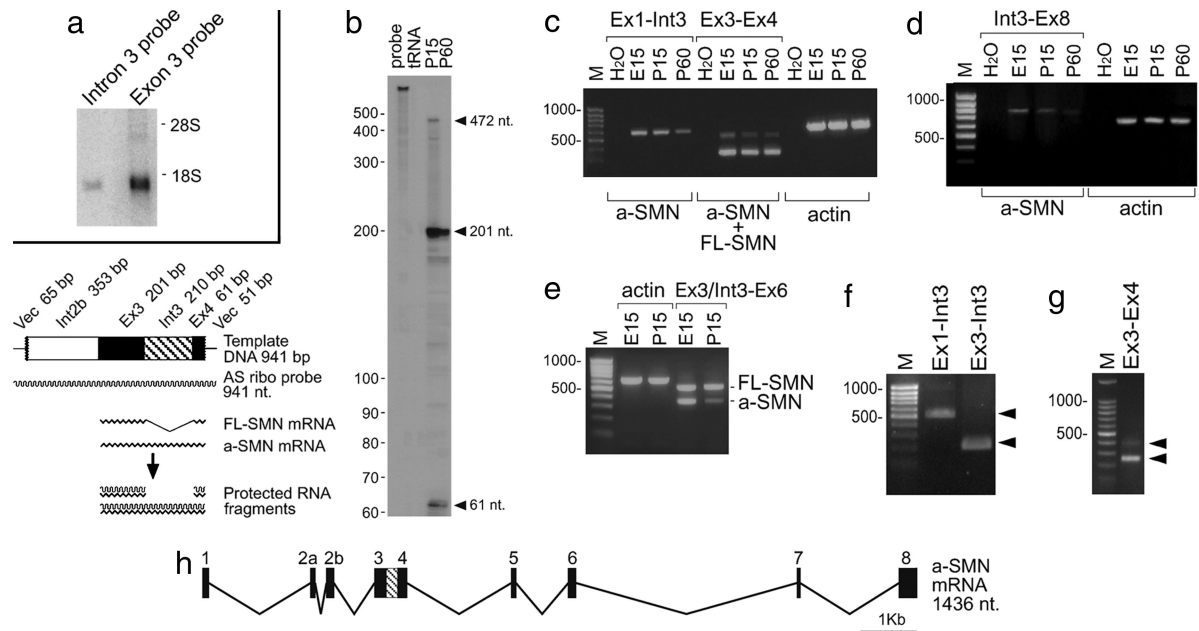
Fig. 1. Molecular characterization of the a-SMN transcript. (*a*) Northern blot analysis, P15 rat spinal cord: an intron 3 probe hybridized to a transcript (left) similar in size to the *FL-SMN* mRNA (right). (*b*) RNase protection assay. The riboprobe and protected fragments are schematically represented (*Left*). Protected fragments specific for *FL-SMN* (201 and 61 nt) and *a-SMN* (472 nt) mRNAs are indicated by arrowheads (*Right*). (*c* and *d*) RT/PCR analysis. The combinations of primers are indicated. Note the two fragments using exon primers flanking the intron 3 sequence (Ex3–Ex4) and the developmental down-regulation of the a-SMN transcript. (*e*) Competitive PCR. A mixture of primers specific for *SMN* exon 3, intron 3, and exon 6 generated two fragments corresponding to a-SMN (372 bp) and FL-SMN (544 bp). (*f* and *g*) RT/PCR, adult human spinal cord. Exon 1/intron 3 and exon 3/intron 3 pairs of primers (*f*) amplified the expected *a-SMN* cDNA fragments (534 and 221 bp). Primers (Ex3–Ex4) flanking the intron 3 sequence (*g*) amplified a-SMN (upper, 396 bp) and FL-SMN (lower, 237 bp) cDNA fragments. (*h*) Schematic diagram of a-SMN mRNA (retained intron 3 is hatched).

human *SMN1* gene. Sequence analysis of >60 clones from NB4 mRNA showed that all clones came from the *SMN1* gene because there was a C at position +6 in exon 7 and a G at position +233 in exon 8. Approximately two thirds of the clones showed exon 5 skipping. These data are unlikely to be biased because primers targeting exons 2b and 3 amplify fragments corresponding to the FL-SMN and Δ7-SMN mRNAs from the *SMN2* gene.

The a-SMN Protein Is Specifically Expressed within the Spinal Cord in Motor Neuron Axons. In-frame stop codons are present in the intron 3 sequences of human, rat, and mouse a-SMN mRNAs shortly after the exon 3/intron 3 boundary (Fig. 2*a*). Therefore, the a-SMN polypeptides are much shorter than the FL-SMN counterparts, with predicted molecular weight of 21.783 kDa in rats (pI: 7.45), 18.448 kDa in mice (pI: 7.59), and 18.865 kDa in humans (pI: 8.53). The amino acid sequence from intron 3 is longer in rats and different in the three species.

We then raised antibodies against the peptides encoded by rat and human intron 3. The rat antibodies highlighted the predicted 23-kDa protein band in spinal cord membranes, which was completely abolished after preincubation with the intron 3 peptide (Fig. 2*b*). The a-SMN protein was detectable only during motoneuronal development and was down-regulated after birth. Western blot (WB) analysis of other neuronal and non-neuronal tissues revealed similar developmental profiles: levels of expression are comparable at E15 in the brain and liver, whereas in the heart they are barely detectable.

The cellular localization was then analyzed by confocal immunofluorescence (IF) (Fig. 2 *c* and *d*) and immunocytochemistry (Fig. 2 *e* and *f*). In the P1 rat spinal cord, the antibody labeled the perinuclear region, external cellular membrane, and dendrites of lamina IX motor neurons (Fig. 2*c*). a-SMN was expressed in axons, with strong signals in the spinal white matter and in axons forming the ventral roots (Fig. 2*d*). a-SMN staining was selective because the

gray matter outside lamina IX was not labeled, and no glial staining was detected. The localization justifies the name adopted for this SMN transcript and protein. The anti-human antibodies stained the perikarya and axons of spinal motor neurons and cortical pyramidal neurons of newborn infants (Fig. 2 *e* and *f*). In WB analysis of human embryonic spinal cords (Fig. 2*g*), two different antibodies specific for human a-SMN revealed the predicted protein band of ≈20 kDa.

The a-SMN Protein Stimulates Axonogenesis. The functional significance of a-SMN was investigated by overexpression experiments in cultured cells. We used constructs encoding unmodified *SMN* cDNAs or tagged at the amino terminus (*tag-SMN*) or fused in-frame to the green fluorescent protein cDNA (*GFP-SMN*). After transfection of *tag-FL-SMN* in NSC34 motor neurons (20), anti-tag antibodies recognized the predicted 41-kDa band (Fig. 3*a*). Anti-SMN antibodies detected the tagged and the 38-kDa endogenous FL-SMN protein. The *tag-FL-SMN* protein accumulated in coarse granules in the cytoplasm and nucleus (Fig. 3*b*). Smaller granules were observed in neurites, with no changes of cell morphology. Expression of the native FL-SMN produced identical results (data not shown). These data are consistent with reported effects of FL-SMN in different cell systems (10, 21, 22).
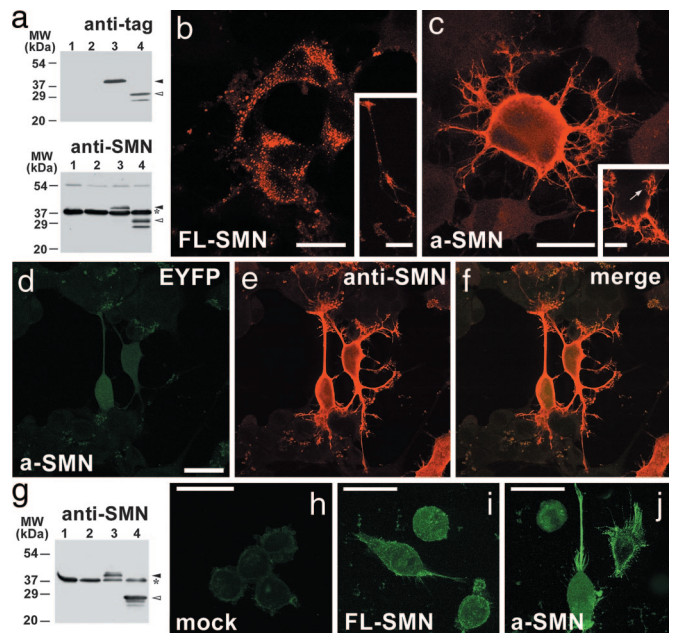
Transfection of NSC34 with *tag-a-SMN* consistently led to the expression of two SMN bands (Fig. 3*a*) recognized by anti-tag antibodies and by anti-SMN antibodies directed against the SMN N terminus (Fig. 3*a*). The 27-kDa band is consistent with the calculated weight of the tagged a-SMN protein, whereas the 29-kDa band suggests posttranslational processing. Transfection of *tag-a-SMN* (Fig. 3*c*) and native *a-SMN* (Fig. 3 *d–f*) dramatically changed NSC34 morphology, inducing filopodia- or neuritic-like extensions. Intensely immunofluorescent neurites radiating out of the perikaryon and touching the cell bodies of neighboring NSC34 cells were often seen (Fig. 3 *c–f*). This did not happen in cells transfected
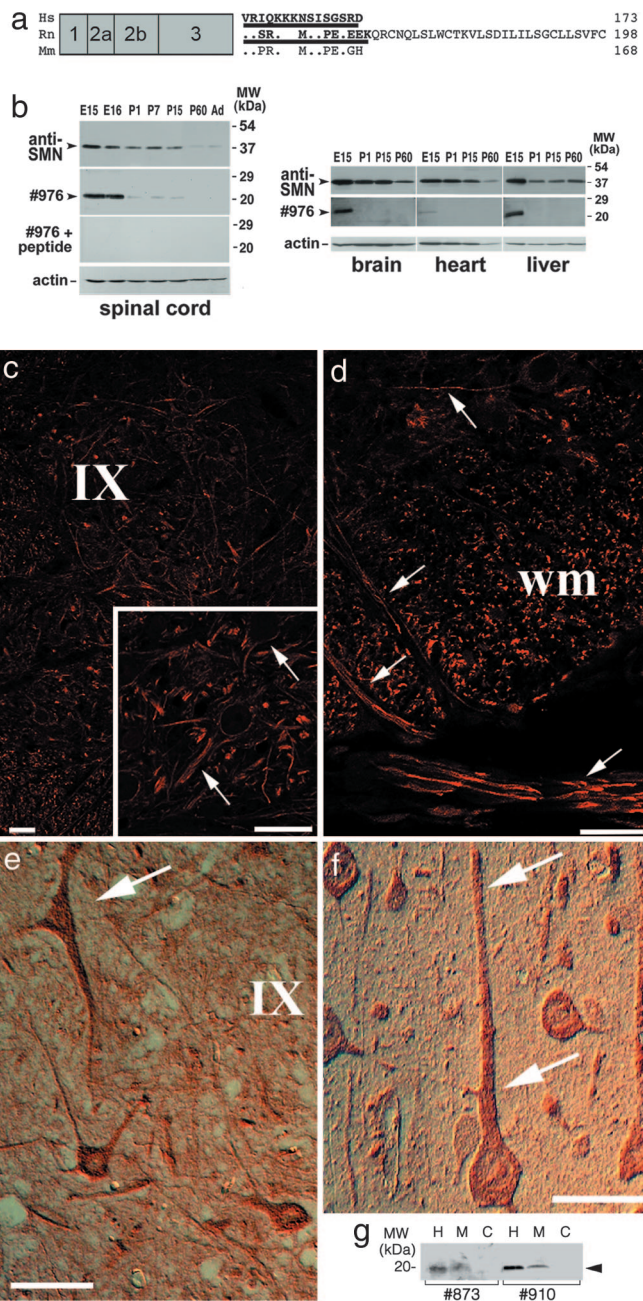
Fig. 2. Expression of the a-SMN protein *in vivo*. (*a*) Primary structure of human, rat, and mouse a-SMN. Intron 3 epitopes recognized by a-SMN antibodies are underlined. (*b*) WB analysis of rat tissues. In the spinal cord (*Left*), the anti-rat a-SMN antibody #976 recognizes a developmentally down-regulated 23-kDa band (arrowhead), which is abolished in preabsorption experiments. Note the similar developmental profile in the brain, heart, and liver (*Right*). All blots were reprobed with an anti-SMN antibody. (*c* and *d*) P1 rat spinal cord. Note the selective a-SMN staining of external cellular membrane and dendrites (arrows in *c*) and axons (arrows in *d*) of lamina IX motor neurons. (*e* and *f*) Developing human spinal motor neurons (arrows in *e*) and cortical pyramidal neurons (arrows in *f*) are intensely a-SMN-immunoreactive. (*g*) WB analysis of human embryonic spinal cord. Note the a-SMN 20-kDa band in the total homogenate (H) and membrane (M) fraction but not in the cytosol (C). (Scale bars: *c* and *d*, 30 μm; *e* and *f*, 50 μm.)

Fig. 3. FL-SMN and a-SMN overexpression. (*a*) WB analysis. Transfected *FL-SMN* (filled arrowheads) and *a-SMN* (open arrowheads) are indicated. Note the two a-SMN bands, suggesting posttranslational processing. (*b* and *c*) NSC34 cells transfected with tagged FL-SMN (*b*) or a-SMN (*c*). Shown is anti-tag antibody. (*b Inset*) Few FL-SMN granules in neurites. (*c Inset*) a-SMN neurites touching neighboring cells. (*d–f*) Transfection of pIRES-EYFP *a-SMN*. Note the newly formed neurites contacting untransfected NSC34 adjacent cells. (*g–j*) Transfection in HeLa. (*g*) WB analysis; protein bands are indicated as above. (*h–j*) Confocal images of mock-transfected (*h*), *FL-SMN*-transfected (*i*), and *a-SMN*-transfected cells (*j*) reacted with anti-F-actin antibody. Lane 1, untransfected cells; lane 2, mock transfection; lane 3, *FL-SMN* transfection; lane 4, *a-SMN* transfection. *, endogenous FL-SMN. (Scale bars: *b*, *c*, and *h–j*, 25 μm; *d–f*, 30 μm; *Insets*, 10 μm.)

with *FL-SMN* or the void vector. The subcellular localization of transfected a-SMN *in vitro* is consistent with the results in motor neurons *in vivo*.

Because NSC34 are already committed to neuronal differentia-

tion (23), we verified whether a-SMN induced newly formed neurites in HeLa, human epithelial cells incapable of axonogenesis. The *tag-FL-SMN*- and *tag-a-SMN*-transfected cells were labeled with an antibody against F-actin, a growth cone marker (24). In basal conditions, HeLa cells have round bodies with no filopodia-like extensions (Fig. 3*h*). Transfection of the *a-SMN* cDNA, but not the *FL-SMN* construct (Fig. 3*i*) or void vector, induced relatively long F-actin-positive cell processes, which surrounded the cell bodies and had in some cases a neuritic morphology (Fig. 3*j*). Thus, a-SMN can induce axonal-like growth even in a non-neuronal context.

We next analyzed the effect of human *a-SMN* (*ha-SMN*) and *FL-SMN* overexpression in NSC34 and HeLa cells (Fig. 4). In WB analysis, *tag-ha-SMN* transfection produced two protein bands, whereas the *GFP-ha-SMN* construct produced a protein band corresponding in size to the sum of the two polypeptides (Fig. 4*a*). A strong effect was evident after overexpression of all types of human *a-SMN* (Fig. 4). *GFP-ha-SMN* was evident at branching points of neurites of NSC34 cells (Fig. 4 *b* and *c*). In HeLa cells, human a-SMN induced striking outgrowth of cellular filopodia, where it was extensively colocalized with F-actin (Fig. 4*f*). These effects were never seen in cells transfected with human FL-SMN (data not shown).

We then analyzed the kinetics of the axonogenic effect of a-SMN. Twelve hours after transfection, NSC34 motor neurons had thick, short neurites surrounded by radiating filopodia (Fig. 5*a*). After 24 h, cells had a multipolar appearance, with longer neurites radiating in all directions (Fig. 5*b*). After 48 h, neurites were fewer but longer (Fig. 5*c*). After 72 h, most motor neurons showed unipolar morphology with single, long axons always surrounded by
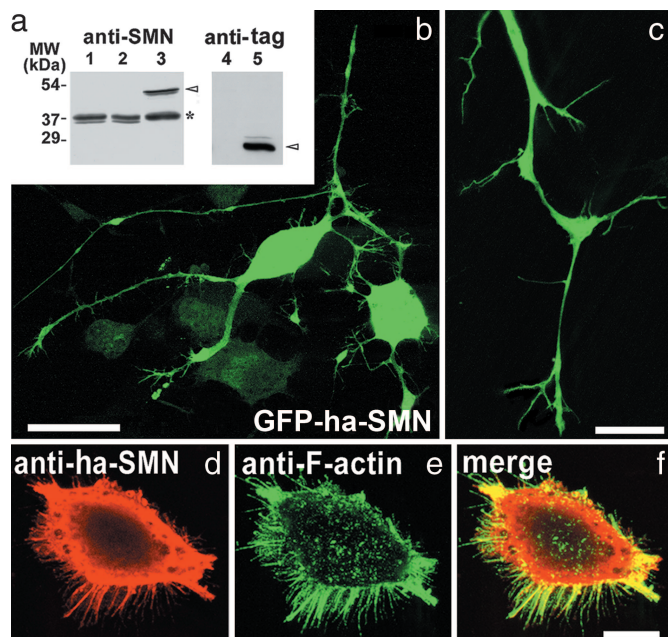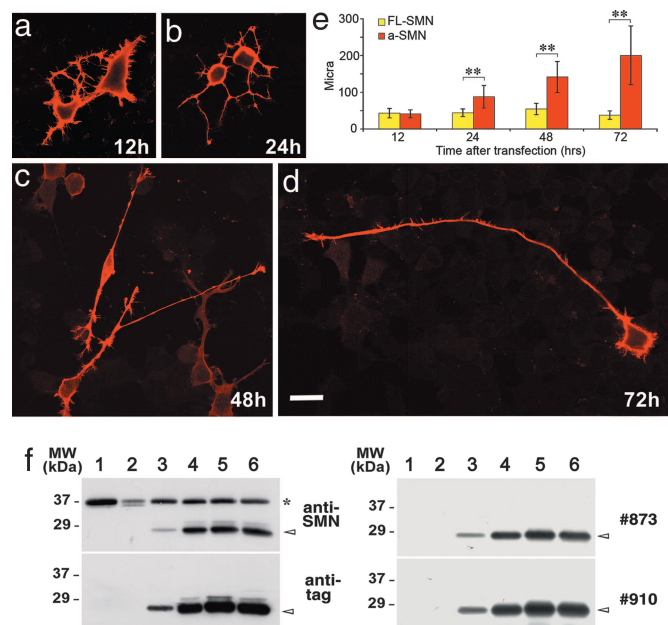
Fig. 4. Human *a-SMN* (*ha-SMN*) overexpression. (*a*) WB analysis in NSC34; GFP-a-SMN (*Left*) and tagged-a-SMN (*Right*) proteins are indicated. Lane 1, untransfected cells; lane 2 and 4, mock transfection; lane 3, *GFP-ha-SMN* transfection; lane 5, tag-ha-*SMN* transfection. *, endogenous FL-SMN. (*b* and *c*) *GFP-ha-SMN* expression in cell bodies (*b*) and neurites (*c*) of NSC34. (*d–f*) Confocal images showing human a-SMN (*d*) (#910 anti-SMN) and F-actin (*e*) colocalization (*f*) in newly formed filopodia of HeLa cells transfected with *ha-SMN*. (Scale bars: *b*, 25 μm; *c–f*, 10 μm.)

Fig. 5. Time course of human a-SMN overexpression. (*a–d*) Confocal images with an anti-tag antibody at 12 (*a*), 24 (*b*), 48 (*c*), and 72 (*d*) h after transfection. (Scale bar: 30 μm.) (*e*) Mean axon length at different time points in *a-SMN* and *FL-SMN* transfected motor neurons. Data are mean ± SD of triplicate wells (seven cells per well). Two-way ANOVA and two-tailed *t* test were used for each *a-SMN/FL-SMN* pair at the different time-points (**, $P < 0.01$). (*f*) WB analysis. Anti-SMN, anti-tag, and #873 and #910 anti-a-SMN antibodies (arrowheads) show the a-SMN progressive synthesis (lower band). Lane 1, untransfected cells; lane 2, mock transfection; lanes 3–6, a-SMN transfection at 12, 24, 48, and 72 h. *, endogenous FL-SMN.

many filopodia (Fig. 5*d*). In NSC34, motor neurons overexpressing FL-SMN axon length did not increase and in fact tended to diminish at late time points (Fig. 5*e*).

There were highly significant differences in the axonal length between the a-SMN and FL-SMN groups ($P = 2.14 \times 10^{-11}$) and as a function of time ($P = 7.77 \times 10^{-9}$) (Fig. 5*e*). The mean cellular perimeter did not differ (data not shown). These data indicate that a-SMN induces *de novo* axonogenesis in a time-dependent fashion. The time course of axonogenesis parallels the synthesis of the tagged 27-kDa a-SMN protein, recognized in WB analysis by anti-SMN, anti-tag, and anti-a-SMN antibodies (Fig. 5*f*). Small amounts of an additional 29-kDa band were produced, suggesting posttranslational processing.

Epitope Mapping of the a-SMN Protein. We then functionally mapped a-SMN by transfecting NSC34 motor neurons with different N-terminally tagged constructs. Overexpression of an a-SMN construct containing an in-frame stop codon after the first start codon did not induce any morphologic change (Fig. 6*a*). The transfection resulted in the synthesis of the mRNA (Fig. 6*g*) but not the relative protein. Overexpression of the intron 3 peptide caused accumulation of large cytoplasmic granules with no changes in cell morphology (Fig. 6*b*). The exon 1/2a peptide accumulated in neuritic extensions but did not affect axon growth (Fig. 6*c*). Forced expression of exon 1/2a/2b or exon 1/2a/2b/3 led to accumulation of the corresponding proteins in neurites and induced axon growth (Fig. 6 *d* and *e*). WB analysis confirmed translation of protein bands of the expected weight from the various a-SMN constructs (Fig. 6*f*). Statistical analysis indicated a highly significant axonogenic effect ($P < 0.0001$) of each a-SMN construct compared with FL-SMN (Fig. 6*h*). Differences among a-SMN, exon 1/2a/2b a-SMN, and exon 1/2a/2b/3 a-SMN were not significant. Thus, synthesis of the a-SMN protein is necessary for axonal sprouting, exon 1/2a sequence is important for axonal localization, and the remaining C

terminus is essential for axonogenesis. Retention of intron 3 is important only to provide the stop codon necessary to produce an axonogenic polypeptide truncated at the exon 3/exon 4 junction. This might explain the differences in amino acid sequences encoded by intron 3 in humans, mice, and rats.

Discussion

We report an *SMN* mRNA from the human and rat *SMN* genes extending from exon 1 to exon 8 but differing from the FL-SMN transcript in the presence of the intron 3 nucleotide sequence. The encoded protein, a-SMN, is much shorter than the FL-SMN counterpart because of stop codons truncating the reading frame shortly after the exon 3/intron 3 boundary. Therefore, FL-SMN and a-SMN have identical N-terminal regions and diverge for the C-terminal tails.

The a-SMN protein is found in neuronal and non-neuronal tissues, albeit at different levels, and clearly shows developmental down-regulation. This finding suggests that it may exert some general function, critical during embryogenesis. As indicated by overexpression experiments in NSC34 and HeLa cells, this function may be related to filopodia extension. This is a general, dynamic process involved in cellular motility and migration, critical during embryogenesis. Axonogenesis is a specialized neuronal function, but it involves cell shape changes similar to those observed during filopodia extension in non-neuronal cells. Thus, some of the mechanisms underlying these processes may be shared. In fact, the similarity between a-SMN's effect in NSC34 motor neurons and HeLa cells suggests a link between axonogenesis and filopodia extension and between these processes and a-SMN.

Our *in vivo* data show that motor neurons are the cells that express a-SMN most intensely in the spinal cord. The predominant subcellular localization in dendritic extensions and axonal fibers in motor neurons *in vivo* completely matches the subcellular localiza-
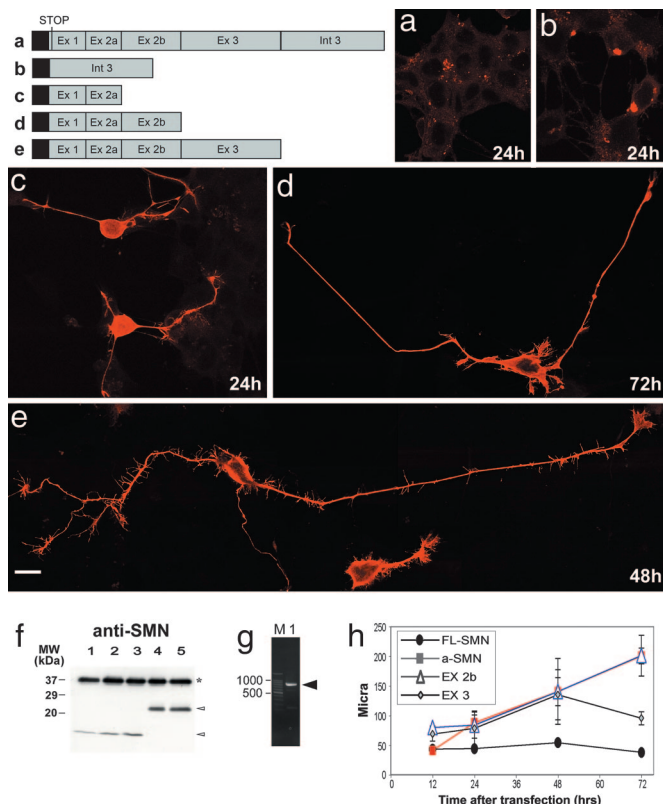
Fig. 6. a-SMN functional mapping. Confocal images (*a–e*) from NSC34 motor neurons transfected with the different N-terminally tagged constructs (upper left). Intervals after transfection are indicated. See text for details. Shown are anti-SMN antibody in *a* and anti-tag antibody in *b–e*. (Scale bar: 30 μm.) (*f*) WB analysis. The anti-SMN antibody reveals the translated a-SMN bands of the expected size (arrowheads). Lane 1, exons 1/2a overexpression (24 h); lanes 2 and 3, exons 1/2a/2b overexpression (24–48 h); lanes 4 and 5, exons 1/2a/2b/3 overexpression (24–48 h). *, endogenous FL-SMN. (*g*) RT/PCR analysis showing mRNA synthesis (arrowhead) after transfection of construct *a*. (*h*) Mean axon length at different times after transfection of FL-SMN, a-SMN, exons 1/2a/2b a-SMN(EX 2b), and exons 1/2a/2b/3 a-SMN(EX 3). Data are mean ± SD of triplicate samples (six cells per well). Two-way ANOVA indicated a significant effect ($P < 0.0001$) of each *a-SMN* construct compared with *FL-SMN*.

tion of a-SMN in transfected NSC34 motor neurons. Therefore, the cellular/subcellular compartmentalization and the expression profile suggest a specific function of the a-SMN protein in developing motor neuron axons. This function may not be limited to motor neurons but might be common to other long projecting neurons in the CNS, given the strong expression in cortical pyramidal neurons.

It has already been proposed that the *SMN* gene plays a role in motor axon development. Suppression of *SMN* expression by means of morpholino antisense oligonucleotides impaired the growth of motor axons in zebrafish (25). Immunocytochemistry revealed SMN in the axons of motor neurons and in the growth cones of cultured neuronal and nonneuronal cells. In these locations, the protein associates with cytoskeletal elements and ribosomal RNA (18, 24, 26). These data have been taken to suggest that FL-SMN controls the axonal transport of messenger RNAs. However, FL-SMN and a-SMN share an identical N-terminal region, and the probes used in those studies were directed against the N terminus or the 5′ sequence of SMN. Thus, these results need to be reconsidered in light of the existence of the a-SMN protein.

SMN exerts its functions by interacting with a variety of proteins in the nucleus (8–10, 27–31) and axons (32–35). Preliminary experiments indicate that cotransfected FL-SMN and a-SMN do not colocalize in NSC34 motor neurons (V.S., D.L., and G.B.,

unpublished work), thus making functional interactions between the two proteins unlikely. a-SMN lacks the self-oligomerization domain (36) present in the C-terminal tail of FL-SMN. The a-SMN domains encoded by exons 2b and 3 that are responsible for axonogenesis may possibly interact with other partner proteins involved in the extension of cellular processes. This is consistent with the colocalization with F-actin in newly formed filopodia reported in the present work. The exons 2b and 3 domains in the FL-SMN protein may be inaccessible to the interacting partners.

Because a-SMN is the product of a disease gene, a key issue is the contribution of the two human *SMN* genes to its production and hence its relevance in the pathogenesis of SMA. On the basis of present knowledge, both *SMN1* and *SMN2* can potentially generate a-SMN. However, an important observation was made in the human cell line NB4, where we demonstrated that a-SMN is transcribed specifically from the *SMN1* gene. This indicates that intron 3 retention is a characteristic of the *SMN1* gene. The mechanism of this selectivity is still not known and difficult to guess, given that the *SMN1* and *SMN2* genes differ only for two polymorphic sites in exons 7 and 8.

NB4 is an acute myeloid leukemia cell line committed along the granulocytic pathway (37) and is unlikely to be useful for experimentally defining the significance of a-SMN in axonogenesis. However, if selective transcription of a-SMN from the *SMN1* gene were a general phenomenon also seen in neurons, the observation may have far-reaching implications for the pathogenesis of SMA. The crucial difference between *SMN1* and *SMN2* believed to be relevant for the SMA phenotype is a C/T transition in exon 7, which disrupts a splice enhancer or creates an inhibitor site (38–41). We propose that transcription of a-SMN from the *SMN1* gene is another determinant in the etiopathogenesis of the disease. Indeed, loss or reduction of a-SMN may be relevant to the SMA phenotype. The localization and striking effect on axon growth are consistent with a-SMN being involved in SMA because the disease primarily affects motor neurons, and motor neuron axons have scant ability to sprout in type I SMA patients (42). More direct data, for instance from spinal cords of human patients and transgenic models (43, 44), are necessary to establish the relation between a-SMN and SMA.

Whatever the role of a-SMN in SMA, its discovery adds unexpected complexity to the biology of the *SMN* gene system and provides a potential determinant of SMA pathogenesis. In a broader perspective, the functional properties of a-SMN in stimulating axonogenesis may be useful in developing new therapeutic strategies based on gene therapy. Recent data from preclinical models indicate that gene transfer delivery to motor neurons is a viable option for the treatment of transgenic models of motor neuron diseases (45, 46).

Methods

RACE and RT/PCR Analysis. Postnatal and embryonic rat spinal cords were quickly removed after scheduled death, in accordance with the "Principles of Laboratory Animal Care" (National Institutes of Health Publication no. 86-23, revised in 1985). Total RNA was extracted and the poly(A)$^+$ RNA fractionated by oligo(dT)-cellulose chromatography. Human spinal poly(A)$^+$ RNA was purchased from BD Biosciences (Franklin Lakes, NJ). The Marathon cDNA amplification kit (BD Biosciences) was used for RACE/PCR, and the GeneAmp RT-PCR core kit (Applied Biosystems, Foster City, CA) and Advantage 2 polymerase mix (BD Biosciences) were used for RT/PCR. The following oligonucleotides derived from the rat *SMN* cDNA (GenBank accession no. U75369) or rat and human genes (GenBank accession nos. NW_047617 and NW_078018) were used: Ex1S (nucleotides 71–96), Ex3S (445–470), Ex4AS (634–653), Ex8AS (1118–1140), Int3S (5558400–5558425), Int3AS (5558481–5558506), hEx3S (237129–237150), hEx4AS (236783–236684), and hInt3S (236815–236838).

Northern Blot and RNase Protection Analyses. Northern blots were done according to standard procedures. Exon 3- and intron 3-specific cDNA probes were radiolabeled by PCR with [α-^{32}P]dCTP. For RNase protection assay, a rat genomic fragment containing 353 bp of intron 2b, intact exon 3 and intron 3, and 61 bp of exon 4 was amplified and cloned in pBluescriptII KS (Stratagene, La Jolla, CA). Antisense riboprobes were synthesized with [α-^{32}P]UTP and hybridized to poly(A)$^+$ RNA (5 μg each) and RNase-digested by using the RPAIII kit (Ambion, Austin, TX). RNA century markers (Ambion) were [α-^{32}P]dUTP-labeled.

Antibodies. Anti-peptide rabbit polyclonal antibodies against the C-terminal region of rat (#937 and #976) or human (#873 and #910) a-SMN were prepared by NeoMPS and used at 1:1,000 dilution. Mouse anti-SMN was purchased from BD Biosciences (anti-SMN, clone 8; diluted 1:1,000 for IF, 1:25,000 for WB analysis), mouse anti-F-actin was purchased from Chemicon (diluted 1:1,000–1:5,000; Temecula, CA), and mouse anti-tag (anti-Xpress and anti-HisG) was purchased from Invitrogen (diluted 1:1,000, Carlsbad, CA).

Western Blot Analysis. Tissues were removed from embryonic, postnatal, and adult rats. Embryonic (15 weeks) human spinal cords were obtained through a protocol for fetal stem cell production and approved by the ethics committee of the Neurological Institute. All tissues were homogenized in buffer containing 20 mM Hepes (pH 7.4), 1 mM DTT, 1 mM EGTA, 0.1 mM PMSF, and Complete (Roche, Indianapolis, IN). Cellular membrane and soluble fractions were obtained by pelleting nuclei at $1,000 \times g$ for 10 min, then centrifuging the supernatant at $100,000 \times g$ for 45 min. Transfected cell cultures were lysed in buffer containing 0.1 M Na-phosphate (pH 7.4), 0.2% Triton X-100, 0.1 mM EDTA, 0.2 mM PMSF, 1 μg/ml aprotinin, and 1 μg/ml leupeptin by three freezing and thawing cycles. The cell lysates were centrifuged at $13,000 \times g$. Protein extracts were separated on SDS/12% PAGE, blotted to nitrocellulose membranes (1 h, 180 mA), and analyzed with ECL.

Histology, Immunocytochemistry, and Immunofluorescence Analysis. After perfusion with 4% paraformaldehyde, rat spinal cords were dissected and postfixed overnight. Human cerebral specimens were obtained from neurosurgery of non-SMA patients and fixed by immersion in 4% paraformaldehyde. Spinal cords and cerebral tissues were cut on a Vibratome. Paraplast-embedded spinal cord of a non-SMA 6-month-old infant was obtained from the Neuropathology Unit of the Neurological Institute and cut with a rotary microtome. Sections were analyzed by immunocytochemistry and IF. Immunocytochemistry slides were analyzed with a Nikon (Florham Park, NJ) Microphot FXA microscope. IF images were acquired on a Bio-Rad (Hercules, CA) Radiance 2100 confocal microscope at 1,024 × 1,024-pixel resolution.

Transfection. Appropriate cDNA fragments were cloned in pcDNA4/HisMaxTOPO (Invitrogen), bicistronic pIRES-EYFP (BD Biosciences), or GFP Fusion TOPO (Invitrogen) expression vectors. Transfection was with Lipofectamine Plus (Invitrogen). Transfected cells were harvested after 6, 12, 24, 48, and 72 h and either used for WB analysis or fixed in 4% paraformaldehyde/4% sucrose for confocal IF.

Cell Measurements and Statistical Analysis. After transfection, the perimeters, areas, and axon lengths of transfected cells were quantified at the different time points (12, 24, 48, and 72 h) by using Laser Sharp 2000 software (Bio-Rad) on confocal images of individual motor neurons. For statistical analysis, triplicate experiments were considered. Data were analyzed by two-way ANOVA and two-tailed t test for the different constructs transfected at the different time points.

1. Pearn J (1980) *Lancet* 1:919–922.
2. Lefebvre S, Burglen L, Reboullet S, Clermont O, Burlet P, Viollet L, Benichou B, Cruaud C, Millasseau P, Zeviani M, *et al.* (1995) *Cell* 80:155–165.
3. Feldkotter M, Schwarzer V, Wirth R, Wienker TF, Wirth B (2002) *Am J Hum Genet* 70:358–368.
4. Lorson CL, Hahnen E, Androphy EJ, Wirth B (1999) *Proc Natl Acad Sci USA* 96:6307–6311.
5. Gennarelli M, Lucarelli M, Capon F, Pizzuti A, Merlini L, Angelini C, Novelli G, Dallapiccola B (1995) *Biochem Biophys Res Commun* 213:342–348.
6. Liu Q, Dreyfuss G (1996) *EMBO J* 15:3555–3565.
7. Battaglia G, Princivalle A, Forti F, Lizier C, Zeviani M (1997) *Hum Mol Genet* 6:1961–1971.
8. Liu Q, Fischer U, Wang F, Dreyfuss G (1997) *Cell* 90:1013–1021.
9. Fischer U, Liu Q, Dreyfuss G (1997) *Cell* 90:1023–1029.
10. Pellizzoni L, Kataoka N, Charroux B, Dreyfuss G (1998) *Cell* 95:615–624.
11. Iwahashi H, Eguchi Y, Yasuhara N, Hanafusa T, Matsuzawa Y, Tsujimoto Y (1997) *Nature* 390:413–417.
12. Strasswimmer J, Lorson CL, Breiding DE, Chen JJ, Le T, Burghes AH, Androphy EJ (1999) *Hum Mol Genet* 8:1219–1226.
13. Simic A, Seso-Simic D, Lucassen PJ, Islam A, Krsnik Z, Cviko A, Jelasic D, Barisic N, Winblad B, Kostovic I, *et al.* (2000) *J Neuropathol Exp Neurol* 59:398–407.
14. Williams BY, Hamilton SL, Sarkar HK (2000) *FEBS Lett* 470:207–210.
15. Pellizzoni L, Charroux B, Rappsilber J, Mann M, Dreyfuss G (2001) *J Cell Biol* 152:75–85.
16. Francis JW, Sandrock AW Bhide PG, Vonsattel JP, Brown RH, Jr (1998) *Proc Natl Acad Sci USA* 95:6492–6497.
17. Kerr DA, Nery JP, Traystman RJ, Chau BN, Hardwick JM (1998) *Proc Natl Acad Sci USA* 97:13312–13317.
18. Pagliardini S, Giavazzi A, Setola V, Lizier C, Di Luca M, DeBiasi S, Battaglia G (2000) *Hum Mol Genet* 9:47–56.
19. La Bella V, Kallenbach S, Pettmann B (2004) *Biochem Biophys Res Commun* 324:288–293.
20. Cashman NR, Durham HD, Blusztajn JK, Oda K, Tabira T, Shaw IT, Dahrouge S, Antel JP (1992) *Dev Dyn* 194:209–221.
21. Cisterni C, Kallenbach S, Jordier F, Bagnis C, Pettmann B (2001) *Neurobiol Dis* 8:240–251.
22. Le TT, Pham LT, Butchbach ME, Zhang HL, Monani UR, Coovert DD, Gavrilina TO, Xing L, Bassell GJ, Burghes AH (2005) *Hum Mol Genet* 14:845–857.
23. Simeoni S, Mancini MA, Stenoien DL, Marcelli M, Weigel NL, Zanisi M, Martini L, Poletti A (2000) *Hum Mol Genet* 9:133–144.
24. Fan L, Simard LR (2002) *Hum Mol Genet* 11:1605–1614.
25. McWhorter ML, Monani UR, Burghes AH, Beattie CE (2003) *J Cell Biol* 162:919–931.
26. Zhang HL, Pan F, Hong D, Shenoy SM, Singer RH, Bassell GJ (2003) *J Neurosci* 23:6627–6637.
27. Paushkin S, Gubitz AK, Massenet S, Dreyfuss G (2002) *Curr Opin Cell Biol* 14:305–312.
28. Young PJ, Day PM, Zhou J, Androphy EJ, Morris GE, Lorson CL (2002) *J Biol Chem* 277:2852–2859.
29. Yong J, Wan L, Dreyfuss G (2004) *Trends Cell Biol* 14:226–232.
30. Carissimi C, Baccon J, Straccia M, Chiarella P, Maiolica A, Sawyer A, Rappsilber J, Pellizzoni L (2005) *FEBS Lett* 579:2348–2354.
31. Grimmler M, Otter S, Peter C, Muller F, Chiari A, Fischer U (2005) *Hum Mol Genet* 14:3099–3111.
32. Giesemann T, Rathke-Hartlieb S, Rothkegel M, Bartsch JW, Buchmeier S, Jockusch BM, Jockusch H (1999) *J Biol Chem* 274:37908–37914.
33. Rossoll W, Kroning AK, Ohndorf UM, Steegborn C, Jablonka S, Sendtner M (2002) *Hum Mol Genet* 11:93–105.
34. Rossoll W, Jablonka S, Andreassi C, Kroning AK, Karle K, Monani UR, Sendtner M (2003) *J Cell Biol* 163:801–812.
35. Sharma A, Lambrechts A, Hao le T, Le TT, Sewry CA, Ampe C, Burghes AH, Morris GE (2005) *Exp Cell Res* 309:185–197.
36. Lorson CL, Strasswimmer J, Yao JM, Baleja JD, Hahnen E, Wirth B, Le T, Burghes AH, Androphy EJ (1998) *Nat Genet* 19:63–66.
37. Pisano C, Kollar P, Gianni M, Kalac Y, Giordano V, Ferrara FF, Tancredi R, Devoto A, Rinaldi A, Rambaldi A, *et al.* (2002) *Blood* 100:3719–3730.
38. Cartegni L, Krainer AR (2002) *Nat Genet* 30:377–384.
39. Cartegni L, Krainer AR (2003) *Nat Struct Biol* 10:120–125.
40. Kashima T, Manley JL (2003) *Nat Genet* 34:460–463.
41. Singh NN, Androphy EJ, Singh RN (2004) *Biochem Biophys Res Commun* 315:381–388.
42. Monani UR, Lorson CL, Parsons DW, Prior TW, Androphy EJ, Burghes AH, McPherson JD (1999) *Hum Mol Genet* 8:1177–1183.
43. Hsieh-Li HM, Chang JG, Jong YJ, Wu MH, Wang NM, Tsai CH, Li H (2000) *Nat Genet* 24:66–70.
44. Monani UR, Sendtner M, Coovert DD, Parsons DW, Andreassi C, Le TT, Jablonka S, Schrank B, Rossol W, Prior TW, *et al.* (2000) *Hum Mol Genet* 9:333–339.
45. Azzouz M, Ralph GS, Storkebaum E, Walmsley LE, Mitrophanous KA, Kingsman SM, Carmeliet P, Mazarakis ND (2004) *Nature* 429:413–417.
46. Azzouz M, Le T, Ralph GS, Walmsley L, Monani UR, Lee DC, Wilkes F, Mitrophanous KA, Kingsman SM, Burghes AH, *et al.* (2004) *J Clin Invest* 114:1726–1731.